KEY FEATURES IMPACTING SOIL-CONDUCTOR LATERAL BEHAVIOUR AS ILLUSTRATED BY CENTRIFUGE TESTS

Mariajose Guevara, University of Western Australia, WA, Australia, mariajose.guevaracastillo@research.uwa.edu.au
James Doherty, University of Western Australia, james.doherty@uwa.edu.au
Phillip Watson, University of Western Australia, phillip.watson@uwa.edu.au
David White, Universities of Southampton and Western Australia, david.white@soton.ac.uk

ABSTRACT

Conductors are a type of pile used during subsea drilling operations to prevent hole collapse and to provide axial support to the well. The response of the conductor to lateral movement, as induced by environmental conditions, contributes to the assessment of fatigue damage of the entire wellhead system. Such assessment requires soil-structure interaction analysis, typically performed by modelling the soil-conductor lateral behaviour as non-linear springs called p-y curves. While bespoke approaches do exist, current industry practice often involves the use of p-y curves given in API RP2GEO, which were originally developed for foundation piles. Recent studies have shown that these curves do not adequately capture the soil-conductor response, especially at small lateral displacements. In addition, no account is given to load-history effects. This paper presents results from centrifuge testing of a rigid length of conductor installed in reconstituted samples of carbonate silt and subject to cycles of lateral displacement, with focus on identifying key features that influence soil-conductor behaviour. The results show that the degraded secant stiffness is impacted by load history – for example, after applying cycles of large amplitude displacement, the secant stiffness at smaller amplitude cycling will be significantly lower than if it had not previously experienced the more onerous loading. Furthermore, pore pressure dissipation between or during cyclic events can result in secant stiffness increasing. The results presented in this paper are part of an ongoing research project, aimed at improving fatigue design of subsea wells.

Keywords: Conductor, p-y curves, load-history, centrifuge testing, secant stiffness, fatigue

INTRODUCTION

Conductors are a critical part of top tensioned riser systems as used for drilling wells for offshore oil and gas exploration and extraction. A typical system is illustrated in Figure 1, showing the riser connected to the drill floor by an upper flexible joint (UFJ) and pulled at the top by a tensioning system on the drilling vessel. Closer to seabed, the riser is connected to a lower flexible joint (LFJ) attached to the lower packages, which are heavy components used to support safe drilling. These lower packages are positioned above the wellhead system, which itself is joined to the conductor and casing system.

During drilling, the vessel may move in response to environmental loads, and this motion translates to the components at the seabed (including the conductor). Under normal operations, the amount of (cyclic) lateral movement of the conductor is small. However, repeated cycling can produce stress cycles at specific locations – "hot spots" – where fatigue may become critical. In stiff soils, the hot spot will typically be located above the seabed; while for soft soils the hot spot may be located below the seabed. Assessing fatigue utilisation of the system is critical for safe design, and requires modelling of soil-conductor behaviour.

Soil-conductor interaction can be analysed using the approaches developed for pile analysis: the conductor is represented as an elastic beam which is restrained laterally by non-linear Winkler springs distributed along its length. Lateral and/or moment loads act at the top of the conductor, and the functions that define the non-linear load-displacement response along the pile are called p-y curves. The curves are defined in terms of the resistance of the soil per unit length of pile (p) in response to a lateral displacement (y), often defined in terms of secant stiffness – which is the gradient of the line that joins the origin with a specific point of the curve.

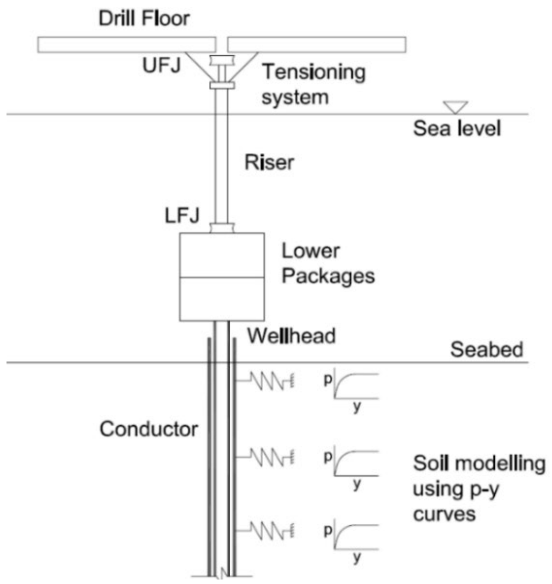

Figure 1. Schematic of a drilling riser system and soil modelling.

The current API RP 2GEO guidelines (API, 2014) recommend monotonic p-y curves that are based on the results of pushover testing performed on piles. It is generally accepted that the API curves underpredict lateral stiffness at modest displacement levels. Given the typical operational displacements at the wellhead of a riser system range between 2.5% and 10% of the conductor diameter (Zakeri *et al.*, 2015), this is particularly important for soil-conductor analysis. Jeanjean (2009) report on a programme of centrifuge experiments and finite element analysis and proposed an alternate monotonic p-y relationship. This was further developed (Jeanjean *et al.*, 2017) by linking the curve to simple shear testing via a scaling method proposed by Zhang and Andersen (2017).

While the monotonic p-y curves provide a backbone response, the behaviour of a riser system is inherently cyclic in nature. More recent studies (Zakeri et al., 2016, 2019) propose a method to account for the effects of cyclic loading. The study found that after 50-100 cycles of lateral loading the p-y response reaches a "steady state stiffness", beyond which no further degradation occurred – and provide recommendations for design. Test results have been presented for a range of soils, although no similar studies have been performed on the carbonate soils found in the North West Region of Australia.

The studies by Zakeri et al. (2016, 2019) do not address load history or potential gain in stiffness due to pore pressure dissipation. Recent experimental testing has shown that these effects may be significant for a range of scenarios (e.g. White and Hodder, 2010; Zhang et al., 2011; Zhou et al., 2019a, 2019b). Moreover, the improvements of applying a load history, or 'whole life', approach in engineering design have been illustrated by Gourvenec et al. (2017), for the case of a fixed subsea mudmat. In that particular study, the foundation area could be reduced by half if the effect of consolidation due to self-weight or preloading was accounted for. Furthermore, the area of the foundation could be reduced even more if the foundation was designed to slide and the effects of load history were considered in the analysis.

Specifically for conductors, Doherty et al. (2019) showed how the p-y response (at a particular value of y) is softer when the conductor was previously subjected to higher amplitude cycling. The study also showed how consolidation between cyclic packages can lead to increased stiffness. Therefore, the unresolved questions are: Could the change in p-y stiffness be relevant for fatigue life estimation of conductors? What factors produce changes in the soil-conductor stiffness?

This paper presents results from centrifuge testing of a rigid length of conductor that was cyclically displaced in reconstituted samples of carbonate silt, focusing on key features observed to affect the response of the soil during the testing.

TEST SETUP

Two centrifuge testing campaigns were conducted in the 1.8 m radius beam centrifuge at the University of Western Australia. The first campaign was conducted on both kaolin clay and carbonate silt, while the second was conducted on carbonate silt only. This paper presents results from the carbonate silt (CS) only.

The carbonate silt has low plasticity (PI ~ 20%) and specific gravity (G_s) of 2.76. Tests were performed at an acceleration of 40 g using a strongbox of internal dimensions of 650 mm long, 390 mm wide and 325 mm height. Samples were prepared with 30 mm of sand to form a base drainage layer, on which the carbonate silt slurry (prepared with moisture content -w- of 140%) was placed. The sample was then spun for ~ 5 days to achieve full consolidation. The final effective unit weight was determined based on the moisture content from core samples extracted from undisturbed locations within each sample, and the specific gravity of the soil grains. The moisture content profile is shown in Figure 2a.

Soil strength (s_u) was determined via a model T-bar penetrometer using a capacity factor $N_{T\text{-}bar}$ =10.5 (Stewart and Randolph, 1991), with tests performed on each day of testing to track any change in strength. A typical strength profile is shown in Figure 2b. The T-bar dimensions were 5 mm in diameter and 20 mm in length, and the tests were performed at a rate of 3 mm/s (to ensure undrained conditions). All tests included a cyclic stage to investigate remoulding, showing a sensitivity of 3.3.

To complement the T-bar tests, a number of soil element (laboratory) tests were performed on carbonate silt samples consolidated in tubes under a vertical pressure representing an embedment depth of 6.0 m. Results from resonant column and monotonic simple shear tests are presented.

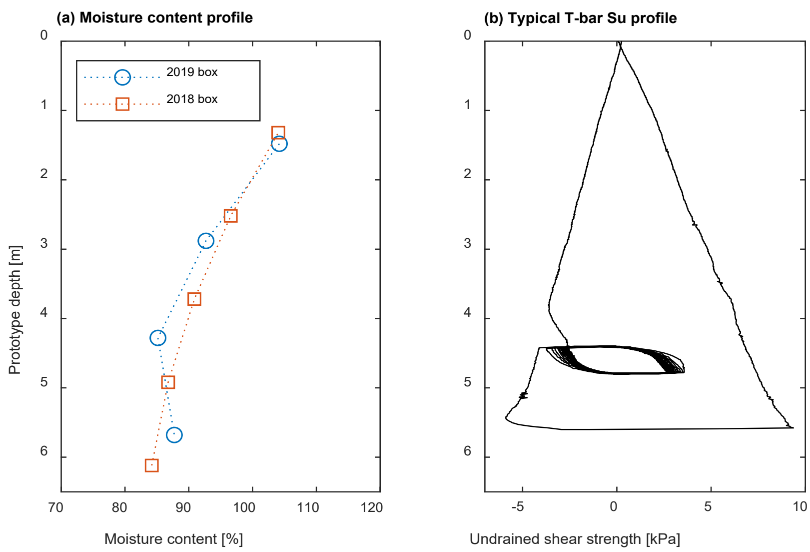

Figure 2.Sample properties: (a) Moisture content profile, (b) Typical undrained shear strength profile from T-bar tests.

The model pile was 3D printed in stainless steel and its diameter and wall thickness were 19.5 mm and 0.95 mm respectively (D/t ratio = 20.5), representing a prototype conductor of 780 mm (30 inch) diameter and 38 mm (1.5 inch) wall thickness. It was instrumented with two pore pressure transducers at different locations (30 mm and 60 mm from the pile tip). The pile was connected to a bending leg, which is used to determine the lateral load H applied to the conductor, based on the difference between moments measured by strain gauges located a specific distance from each other. The displacement and rotation of the pile were measured using two lasers and a flat plate bracket as a target. For the first campaign, an extension was used between the conductor and the bending leg to ensure that the deeper embedment would be achieved. The diagram of the setup for both campaigns is shown in Figure 3.

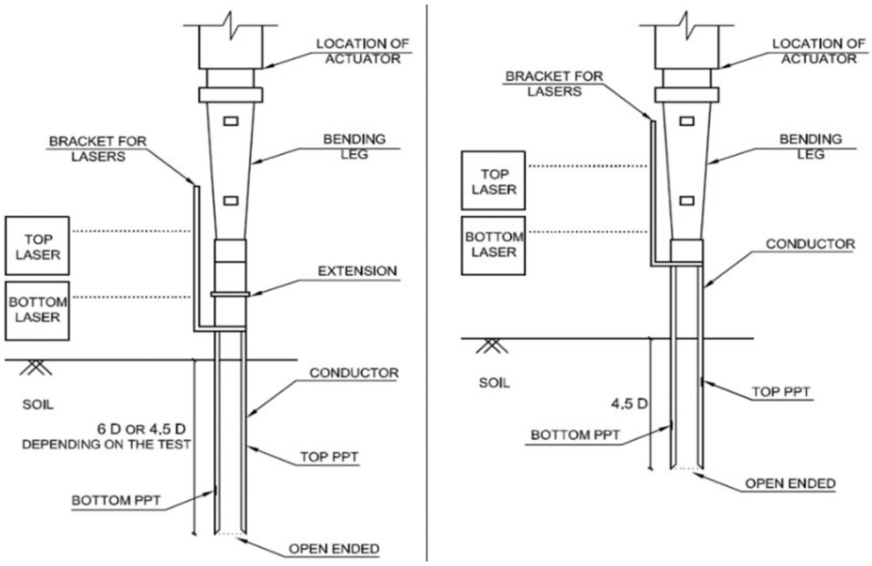

Figure 3. Diagram of test setup: (a) First campaign setup: (b) Second campaign setup.

The hollow piles were installed in flight. A total of 8 tests were performed per sample, with individual test sites separated by sufficient distance to avoid interaction effects (at least 6D from each other and from the walls of the box in the direction of loading). Two different embedment depths of 4.5D and 6D, where D is the pile diameter, were adopted for the first set of tests, while only one embedment depth (4.5D) was used in the second set of tests. No plugging was anticipated for these embedment depths. A wait period of 2.15 hours (model time) separated the installation process from the start of lateral loading, to allow excess pore pressure generated during installation to dissipate. The typical dissipation percentage was between 80% and 90% and the representative c_h of the sample is 4 m^2/year. The wait period was initially estimated based on the solution given by Randolph and Wroth (1979) and subsequently confirmed by monitoring of the pore pressure transducers.

All the tests were displacement controlled at the actuator level. The pile was practically rigid for the range of loads applied. However, there was a very small amount of compliance in the connection of the pile and the bending leg. This was accounted for by developing a relationship between the applied load and the pile rotation (measured with the two lasers), which was then used to determine the pile lateral displacement at 50% of the penetration depth.

TESTING PROGRAMME

During the first campaign, most testing comprised episodes of displacement-controlled cyclic motion followed by a pore pressure dissipation (i.e. consolidation) period. The test sequences and descriptions are shown in Table 1. The post-episode pore pressure dissipation was assessed based on the Osman and Randolph (2012) solution for consolidation around a laterally loaded pile, and time periods were selected to achieve around 75% dissipation. The Osman and Randolph (2012) solution was also used to determine the time frame for which an episode could be considered effectively undrained (≤ 25% dissipation), and when the pore pressure dissipation effects would start to influence the response during an episode.

Table 1. Test type and description

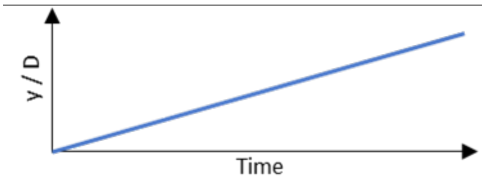	**Type 1 (Campaign 1):** *Monotonic test*. Test to determine lateral capacity (H_{ult}) for comparison to cyclic testing.
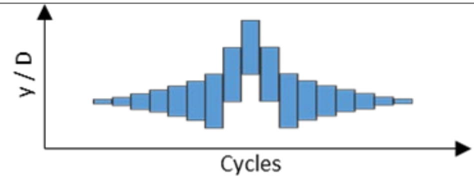	**Type 2 (Campaign 1):** *Small to large amplitude test*. Continuous cycling via packets of 150 cycles at constant peak-to-peak (P2P) amplitudes increasing from 0.01D to 0.16D, followed by cyclic loading around an offset displacement. The pile was then "unloaded" via matching cyclic packets.
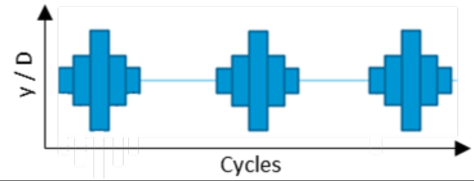	**Type 3 (Campaign 1):** *Undrained 2-way loading.* Episodes of 2 way cyclic loading separated by periods of pore pressure dissipation. Each episode consisted on 5 individual packets of 100 cycles each, ranging from 0.04D to 0.16D.
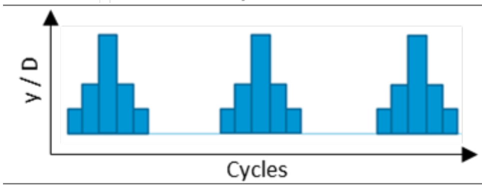	**Type 4 (Campaign 1):** *Undrained 1-way loading.* Episodes of 1 way cyclic loading, using P2P amplitudes and pore pressure dissipation periods comparable to Type 3.
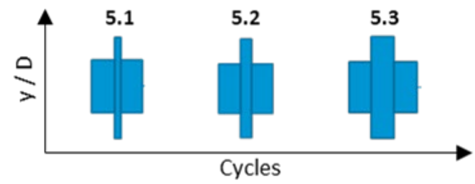	**Type 5 (Campaign 2):** *Impact of higher cycling*. Types 5.1, 5.2 and 5.3 represent individual tests, each performed in new (undisturbed) test locations. Each test comprises 400 cycles at 0.08D, with a higher amplitude (0.12D) event added at the middle. The number of high amplitude cycles varied between 2 (Type 5.1), 20 (Type 5.2) and 200 (Type 5.3)
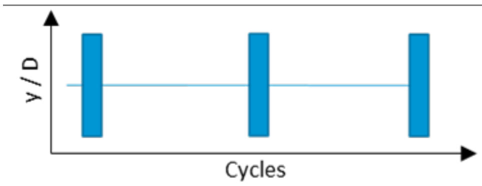	**Type 6 (Campaign 2):** *Undrained 2-way loading*. Episodes of 200 cycles of 0.12D (2-way P2P amplitude) with pore pressure dissipation periods in between.
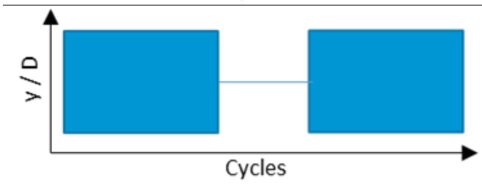	**Type 7 (Campaign 2):** *Long term cyclic response*. Comprised two packages of 2 way loading at 0.12D for 10,000 cycles, with pore pressure dissipation in between.

RESULTS AND DISCUSSION

Results from the centrifuge testing are examined via changes in a normalised cyclic secant stiffness (K). As will be shown, the secant stiffness varied with loading and dissipation histories, and hence there is no "steady state" value. Accordingly, we have reported K at different times, defined as:

$$K = \frac{H/H_{ult}}{y/D}$$

[1]

where H is the cyclic range of horizontal load (representing the integrated response of the distributed soil pressure, p, along the length of the pile); H_{ult} is the measured monotonic lateral capacity from Test 1; D is the pile diameter and y is the lateral displacement at mid embedment depth of the conductor.

A plot of H and displacement at the actuator level vs time can be seen in Figure 4a, for the first 2 episodes of test Type 3 at 4.5D embedment depth. The figure also shows the first and last cycle of packets 2, 3 and 4 highlighted in red, green and magenta, respectively, for the first episode of the test. The shear vs displacement at mid-embedment depth of these highlighted cycles can be observed in Figure 4b.

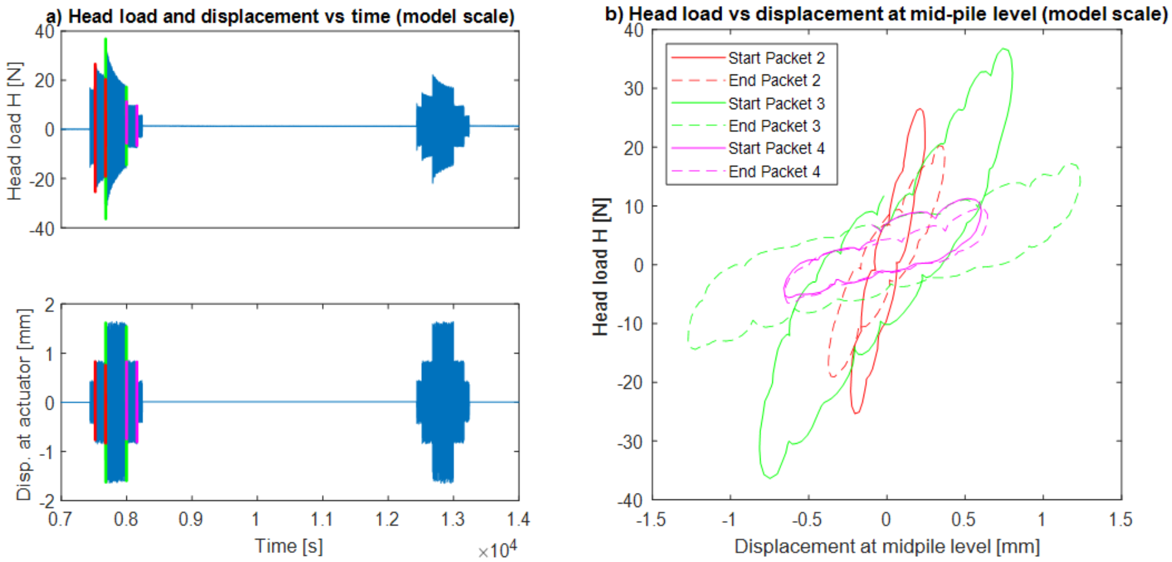

Figure 4. Data from test Type 3 at 4.5 D embedment depth: a) Head load and displacement at the actuator level vs time; b) Head load vs displacement at mid-embedment level for the start and end cycle of the second, third and fourth packets of loading.

Stiffness degradation under cyclic loading

Figure 5 (left and bottom axis) presents K against y/D, where the reported K is from the final cycle of each packet of the increasing amplitude part of the first episode of test Type 2, 3 and 4. The results show that K decreased with increasing y/D, consistent with previous studies. Also shown is the secant shear modulus (normalised by G_{max}) of the carbonate silt as obtained from resonant column and monotonic simple shear (fast and slow) testing against shear strain scaled by a factor of 1.6 (right and bottom axis).

The depth averaged G_{max} for 6D and 4.5D embedment values are 4.73 MPa and 3.55 MPa, respectively. These were estimated by extrapolating the results from resonant column and bender element tests to the mean effective stress at mid-pile level, and assuming a K_0=0.6.

There are clear similarities in the data. This is subject of ongoing work, and broadly consistent with approaches such as the p-y scaling framework proposed by Zhang and Andersen (2017), and suggests that it may be possible to evaluate the cyclic p-y response of conductors from soil element testing.

The effect of prior cycling on stiffness

Test Type 2, 3 and 4 also include stages where the cyclic amplitude was decreased (after being fully degraded at a higher cyclic displacement level), and the results are shown on Figure 6.

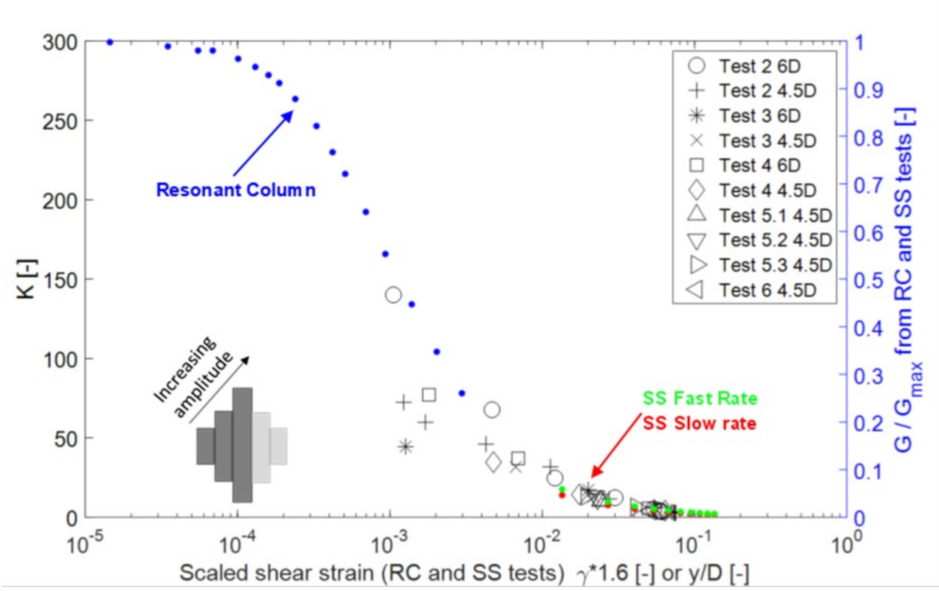

Figure 5. Normalised secant stiffness (K) vs cyclic amplitude from packages of increasing amplitude; and comparison with response from soil element tests.

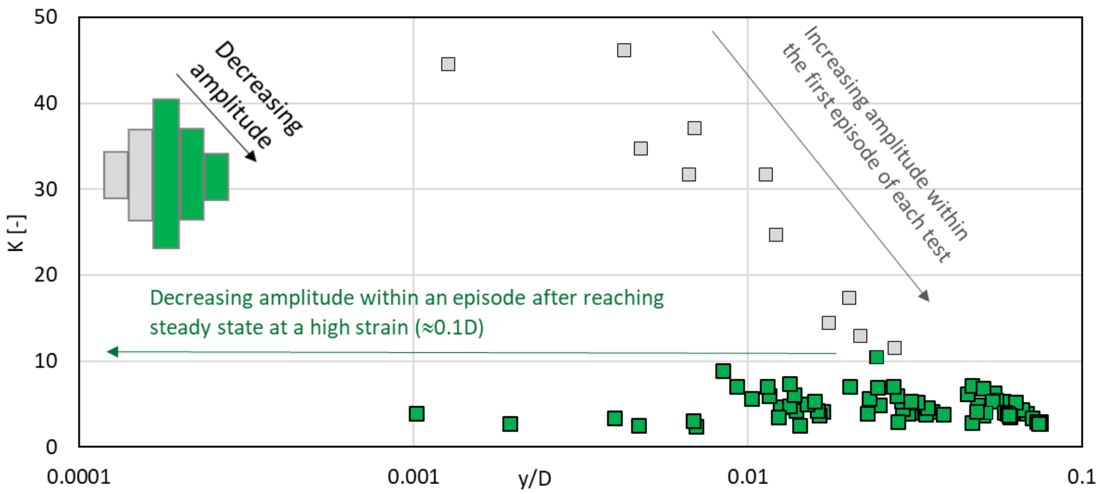

Figure 6. Variation in secant stiffness (K) between rising and falling cyclic amplitude phases.

The results show that the degraded stiffness does not recover when cycling at lower amplitudes. This has the practical implication that once subjected to sufficient cycles at a higher amplitude, subsequent cycles with lower amplitude will have a lower stiffness than predicted from a "steady state" model based on tests with no previous higher amplitude cycles.

Other tests provide an indication of the loading required to cause degradation that will influence subsequent cycles. This is a subject of ongoing study, but some initial clues are provided from test Type 5.1, 5.2 and 5.3 as shown in Figure 7. Each test comprises 400 cycles at 0.08D, with a number of high amplitude cycles (0.12D) added at the middle. The number of larger ("disrupting") cycles was varied between 2, 20 and 200. The results show that changes in stiffness following the "disrupting" high amplitude packet depend on the number of high amplitude cycles – for a packet of 200 high amplitude cycles, the stiffness for subsequent smaller amplitude cycles does not return to its original stiffness, while fewer cycles did not lead to the same level of degradation. This suggests that the cyclic stiffness at a given amplitude depends on cyclic loading history and is a function of the cumulated displacement, and the amplitude of the displacements.

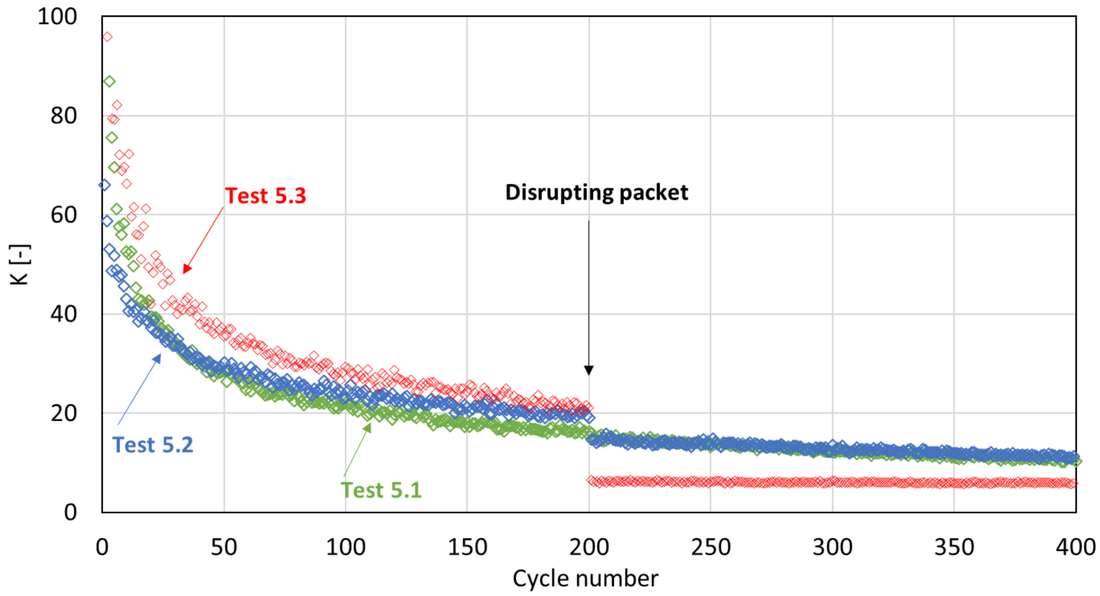

Figure 7. Normalised secant stiffness (K) vs Number of cycles for tests of a packet of 0.05D amplitude disrupted by 2 (Test 5.3), 20 (Test 5.1) and 200 (Test 5.3) cycles of 0.08D.

Recovery in stiffness due to dissipation of excess pore pressure

The regain in stiffness due to pore pressure dissipation is demonstrated from the Type 6 results, as shown in Figure 8. A total of 8 individual episodes of 200 cycles (at 0.12D) were applied, with pore pressure dissipation between each episode resulting in a reduction in excess pore pressure of approximately 75%. During episodes of cyclic motion, the stiffness decreases due to the build-up of excess pore pressures – but after a period of reconsolidation the subsequent stiffness is higher. At the end of episode 8, the degraded (final cycle) stiffness (K = 12) was more than double that seen in the first episode (K = 5).

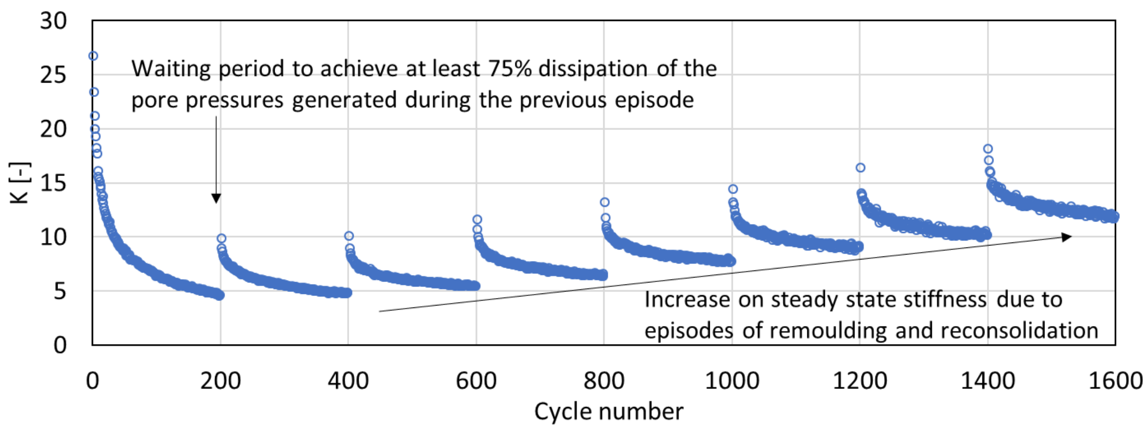

Figure 8. Normalised secant stiffness vs number of cycles for episodes of 200 cycles of amplitude 0.08D at mid-pile level separated by a consolidation period

An alternate way to explore the change in stiffness due to pore pressure dissipation is to track changes in stiffness under long term cyclic loading. Results from a Type 7 test are plotted on Figure 9, and show that after the initial period of (undrained) softening, the stiffness begins to increase. A period of dissipation leads initially to a stronger gain in stiffness, which quickly degrades back to the long-term rising trend. At the end of cycling, the stiffness is roughly half the initial (monotonic) stiffness and 4 times greater than the minimum degraded value. The results are plotted against dimensionless time to make them comparable to different soil types with different horizontal coefficients of consolidation (c_h). For soils with a low c_h this regain in strength might be less significant for the drilling operation itself. However, soils with higher c_h might experience a varying stiffness during the drilling operation, which could affect the fatigue life of the conductor. Changes in stiffness will alter the distribution of lateral load down the pile. In turn, this may cause fatigue hot spots to migrate upward or downward, smearing the damage. Such hotspot migration is not captured in fatigue assessments that consider only a single lateral stiffness that does not change throughout the drilling campaign.

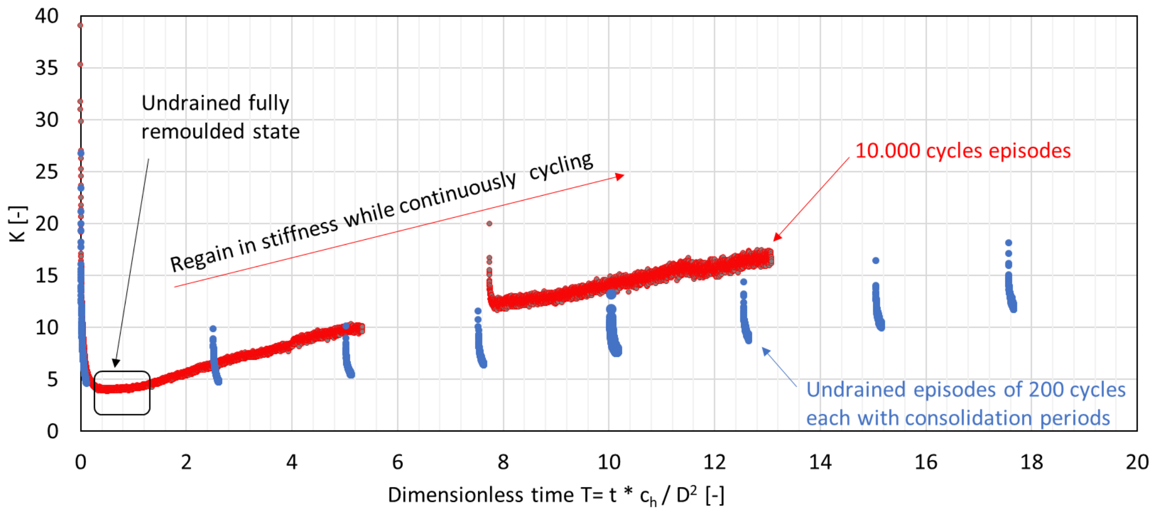

Figure 9. Normalised secant stiffness vs prototype time for episodes of 200 cycles and 10000 cycles of amplitude 0.08D (mid-pile level) separated by periods of consolidation.

Also shown on Figure 9 are the results from Type 6 testing. It is interesting to note that the initial stiffness after dissipation is broadly consistent with the long-term trend in Type 7, but that this value degrades with cycling.

SUMMARY AND CONCLUSIONS

For undrained cyclic loading at given amplitude, there is a minimum (or fully degraded) stiffness that is typically reached after a few hundred cycles, provided that the soil has not experienced higher strains. However, this stiffness does not remain “steady” with time, even when cycling continuously. Accordingly, changes in stiffness may occur during drilling operations, which could affect the fatigue life of the conductor – and should be considered.

Similarities between the shear modulus behaviour from soil element tests and the undrained normalised secant stiffness of p-y curves are shown in Figure 5, suggesting these may be linked for design purposes - although more tests are required to confirm this hypothesis.

Experimental testing has shown that the undrained stiffness K depends on the maximum cyclic amplitude the soil has experienced, and the amount of cycles that are applied. Periods of consolidation also strongly influence conductor stiffness.

Current approaches and guidelines do not take the ‘whole life’ load history into account when determining the soil-conductor behaviour for fatigue analysis, yet this may impact on the fatigue life estimation. This paper has shown that load history has an effect on the stiffness of conductor p-y curves, through degradation and consolidation effects. This work is part of a broader research project conducted at UWA which aims to understand better the ‘whole life’ p-y behaviour and the resulting impact on conductor fatigue life estimation.

ACKNOWLEDGEMENTS

This work was supported by the ARC Industrial Transformation Research Hub for Offshore Floating Facilities which is funded by the Australian Research Council, Shell Australia Woodside Energy, Bureau Veritas and Lloyds Register Group (IH140100012). The third and fourth authors also acknowledge support from Shell Australia via the Shell Chair in Offshore Engineering at UWA.

REFERENCES

API (2014) *Recommended Practice for Geotechnical and Foundation Design Considerations - API RP 2GEO*. 2nd edn. American Petroleum Institute.

Doherty, J., White, D. J., Watson, P. G. and Grime, A. (2019) 'Life cycle changes in p-y stiffness for a conductor pile installed in carbonate silt', in *VSOE 2018: Proceedings of the 1st Vietnam symposium on advances in offshore engineering*. Singapore: Springer, pp. 362–368.

Gourvenec, S. M., Stanier, S. A., White, D. J., Morgan, N., Banimahd, M. and Chen, J. (2017) 'Whole-life assessment of subsea shallow foundation capacity', in *Offshore Site Investigation and Geotechnics 2017 Conference Proceedings*. London: Society for Underwater Technology, pp. 787–795.

Jeanjean, P. (2009) 'Re-Assessment of P-Y Curves for Soft Clays from Centrifuge Testing and Finite Element Modeling', in *Offshore Technology Conference*. Houston, p. 23.

Jeanjean, P., Zhang, Y., Zakeri, A., Andersen, K. H., Gilbert, R. and Senanayake, A. (2017) 'A framework for monotonic p-y curves in clay', in *Proceedings of the 8th International Conference of Offshore Site Investigation and Geotechnics*. London, pp. 108–141.

Osman, A. S. and Randolph, M. F. (2012) 'Analytical Solution for the Consolidation around a Laterally Loaded Pile', *International Journal of Geomechanics*, 12(3), pp. 199–208.

Randolph, M. F. and Wroth, C. P. (1979) 'An Analytical Solution for the Consolidation Around a Driven pile', *International Journal for Numerical and Analytical Methods in Geomechanics*, 3(3), pp. 217–229.

Stewart, D. P. and Randolph, M. F. (1991) 'A new site investigation tool for the centrifuge', in *Proceedings of the International Conference on Centrifuge Modelling, Centrifuge '91*. Balkema, Rotterland, Netherlands, pp. 531–538.

White, D. J. and Hodder, M. (2010) 'A simple model for the effect on soil strength of episodes of remoulding and reconsolidation', *Canadian Geotechnical Journal*, 47(7), pp. 821–826.

Zakeri, A., Clukey, E. C., Kebadze, E. ., Jeanjean, P., Walker, D., Piercey, G., Templeton, J. S., Connelly, L. and Aubeny, C. (2015) 'Recent Advances in Soil Response Modeling for Well Conductor Fatigue-Analysis and Development of New Approaches', in *Offshore Technology Conference*. Houston, p. 30.

Zakeri, A., Clukey, E. C., Kebadze, E. B. and Jeanjean, P. (2016) 'Fatigue analysis of offshore well conductors: Part I – Study overview and evaluation of Series 1 centrifuge tests in normally consolidated to lightly over-consolidated kaolin clay', *Applied Ocean Research*, 57, pp. 78–95.

Zakeri, A., Sturm, H. and Jeanjean, P. (2019) 'Validation and Extension of Soil Response Framework for Fatigue Analysis of Offshore Wells and Piles', in *Offshore Technology Conference*, p. 26.

Zhang, C., White, D. and Randolph, M. (2011) 'Centrifuge Modeling of the Cyclic Lateral Response of a Rigid Pile in Soft Clay', *Journal of Geotechnical and Geoenvironmental Engineering*, 137(7), pp. 717–729.

Zhang, Y. and Andersen, K. H. (2017) 'Scaling of lateral pile p-y response in clay from laboratory stress-strain curves', *Marine Structures*. Elsevier, 53, pp. 124–135.

Zhou, Z., O'Loughlin, C. D. and White, D. J. (2019) 'An effective stress analysis for predicting the evolution of SCR–seabed stiffness accounting for consolidation', *Géotechnique*, 0(0:0), p. 20. doi: 10.1680/jgeot.18.P.313.

Zhou, Z., O'Loughlin, C. D., White, D. J. and Stanier, S. A. (2019) 'Improvements in plate anchor capacity due to cyclic and maintained loads combined with consolidation', *Géotechnique*, 0(0:0), p. 18. doi: https://doi.org/10.1680/jgeot.19.TI.028.